Dipole-dipole interaction in the near-resonant Kapitza-Dirac effect

P. Pax, G. Lenz, and P. Meystre
Optical Sciences Center, University of Arizona, Tucson, Arizona 85721
(Received 4 November 1994)

We study the near-resonant Kapitza-Dirac diffraction of two atoms interacting via the dipole-dipole interaction within the framework of an effective one-dimensional model. We concentrate mostly on the Stern-Gerlach regime of diffraction, where the atomic wave functions are sufficiently well localized that a good physical understanding of the system dynamics in terms of local potentials can be achieved. In general, the dipole-dipole interaction can lead to substantial modifications of the Stern-Gerlach diffraction pattern. We find in particular that under appropriate conditions, bound states of the atomic system can be established, with the two atoms separated by a distance of the order of hundreds of nanometers. However, spontaneous emission eventually destroys the binding between these states via a heating mechanism somewhat similar to strong-field Sysiphus heating. In this respect, the behavior of the "diatom" bound state under the influence of spontaneous emission is similar to that of the atomic solitons predicted to occur in near-resonant Kapitza-Dirac diffraction in the framework of nonlinear atom optics.

PACS number(s): 42.50.Vk

I. INTRODUCTION

The diffraction of atoms by the periodic structure provided by a near-resonant optical standing wave, the near-resonant Kapitza-Dirac effect, is one of the central tenets of atom optics. This problem has been studied in much detail in the past, both theoretically and experimentally, and the various diffraction regimes that can be achieved are well understood [1,2]. The transition from a diffractive to a diffusive regime of interaction as a function of the rate of spontaneous emission has also been analyzed [1–4]. The situation where the optical field needs to be treated quantum mechanically [5–9], a topic of much current theoretical activity, might lead to the development of new techniques to investigate subtle aspects of quantum mechanics, such as the generation of entangled states and measurement theory.

In parallel to these developments, progress in atomic cooling permits one to reach temperatures below the so-called recoil limit, where the atomic thermal de Broglie wavelength becomes larger than the wavelength of the light used to carry out the cooling [10,11]. Moderate to large atomic densities of such ultracold atoms can now be achieved. It is hoped to eventually reach temperatures and phase-space densities such that collective effects such as Bose condensation can be demonstrated [12]. Even before reaching this extreme regime, however, it is reasonable to expect the onset of some evidence for collective effects. This is true in particular in the case of the near-resonant Kapitza-Dirac effect, where the atoms are driven by an electromagnetic field, and hence are subject to the long-range dipole-dipole interaction between ground and excited states [13]. This interaction has a range of the order of an optical wavelength and is expected to start playing a significant role already at moderate densities. This is in contrast to the van der Waals interaction between ground state atoms [14], which is short range and of considerable importance in Bose condensation.

Attempts to understand the effects of these long-range forces on dense clouds of magneto-optically trapped ultracold atoms already constitute an actively pursued field [15–18]. An interesting question under these conditions is to quantify the limitations these forces impose on the ultimately achievable temperatures and densities in magneto-optical traps. The description of observed trap losses [19–22] by means of semiclassical scattering methods or optical Bloch equations shows mixed results so far. There are indications that it is crucial for the understanding of the dynamics of ultracold atoms in light fields to analyze the full problem, including translational and internal degrees of freedom, quantum mechanically [23,24]. But probably the most intriguing consequence of these long-range forces under the low temperatures and moderate to high densities under consideration is the appearence of genuine quantum mechanical many-body effects. Efforts to include them in quantum field theories of ultracold atoms are now being carried out both in the context of Bose-Einstein condensation [25–29] and in atom optics [30–34]. In particular, such theories lead to effective single-atom dynamics in the mean field of the other atoms that are typically nonlinear, leading to the possibility of nonlinear atom optics.

Many-body theories always contain a number of approximations and ansatz whose validity is difficult to assess. Hence, it is necessary to complement them with the study of simple models including just a few atoms, but treated fully quantum mechanically. In addition, such models yield physical intuition on the dynamics of two-body interactions which is complementary to that gained from many-body theories. Progress along these lines has recently become possible thanks in large part to the development of Monte Carlo wave function simulation techniques [35,36]. Applications of such models to

the study of cold collisions in lasers fields [24], as well as of the effects of the resonant dipole-dipole interaction in velocity-selective coherent population trapping [37] and in polarization gradient laser cooling [38] have recently been presented. In this paper, we discuss the diffraction of two undistinguishable atoms by a classical standing-wave field, including spontaneous emission as well as the effects of the dipole-dipole interaction. In addition, we use properly symmetrized initial conditions to take into account the effects of quantum statistics, in case the overlap between the atomic wave functions becomes important.

Section II presents our model and outlines the description of the interaction between the atoms and the standing-wave field, as well as their interaction with the vacuum modes of the electromagnetic field. We review how this interaction leads to both spontaneous decay and the appearance of a dipole-dipole interaction between ground and excited atoms. The atomic master equation resulting from the adiabatic elimination of the vacuum modes of the electromagnetic field is then presented. Unfortunately, the size of presently available computers forbids a direct numerical solution of this equation. Instead, we use a Monte Carlo wave functions technique, whose implementation is discussed in Sec. III, to simulate the resulting atomic dynamics. Section IV presents selected results from our numerical experiments, and demonstrates that the dipole-dipole interaction can have significant effects on atomic diffraction. These results are given a simple physical interpretation in terms of local potentials that are a generalization of the usual dressed states basis of quantum optics that includes the dipole-dipole interaction. Finally, Sec. V is a summary and conclusion.

II. THE MODEL

We consider two undistinguishable bosonic two-level atoms in interaction with a linearly polarized standing-wave classical laser field, as well as with the vacuum modes of the electromagnetic field. We assume that the standing wave is along the x direction, along which the atomic motion is quantized. However, the atomic motion perpendicular to this axis, in the direction of propagation of the atomic beam, is treated classically. Physically, this can be justified by considering a transversely cooled atomic beam traveling with a velocity v_z much larger than the atomic recoil velocity $v_{rec} = \hbar q/M$, where q is the wave number of the standing-wave field and M is the atomic mass. Technically, this allows the significant simplification of effectively dealing with a one-dimensional problem. The two-level atoms have a Bohr transition frequency ω_0 between their excited level $|e\rangle_i$ and ground level $|g\rangle_i$, $i = 1, 2$. In a frame rotating at the laser frequency ω_L, their interaction with the laser field is given in the electric dipole and rotating-wave approximations by

$$H = \sum_{i=1}^{2} \frac{\hat{p}_i^2}{2M} - \frac{\hbar\delta}{2}\hat{\sigma}_{3i} + \hbar\mathcal{R}\cos(q\hat{x}_i)\hat{\sigma}_{1i}. \tag{1}$$

Here $\hat{p}_i$ is the longitudinal center-of-mass momentum operator of the ith atom (i.e., along the standing-wave axis) and $\hat{x}_i$ its position operator, with $[\hat{x}_i, \hat{p}_j] = i\hbar\delta_{ij}$, $\delta = \omega_L - \omega_0$ is the detuning of the laser field with respect to the atomic transition frequency, and $\mathcal{R}$ is the laser Rabi frequency at the antinodes of the standing wave. The operators $\hat{\sigma}_{1i}$ and $\hat{\sigma}_{3i}$ are standard Pauli pseudospin operators for the ith particle. In the absence of two-body (or more generally many-body) interactions, the difference between the one-atom and two-atom near-resonant Kapitza-Dirac effect appears solely in the initial condition, which must be properly symmetrized in the latter situation [39].

Before proceeding, a few words of caution are called for in order to understand the limitations and assumptions made in writing down our model. When using the electric dipole form of the field-atom interaction the resulting Hamiltonian contains a contact term [40]. It is ignored in our Hamiltonian because the "length scale" of this contact term is the Bohr radius, and we assume that the density is low enough that this term is irrelevant. Consequently, we never encounter the difficulty of including van der Waals, fine or hyperfine interactions, as seems necessary to explain trap losses due to ultracold collisions. In addition we assume that our sample is optically thin, otherwise the field and matter equations would have to be solved self-consistently.

In the Born-Markov approximation [41], the coupling of the atoms to the vacuum modes of the electromagnetic field leads to two effects: the first one is spontaneous emission, as would be the case for a single atom, and the second one is the appearance of a dipole-dipole interaction that couples one of the atoms in its excited electronic state to the other in its ground electronic state. Its physical origin is the reabsorption by one of the atoms of a photon spontaneously emitted by the other.

We do not reproduce the derivation of the appropriate two-atom master equation, which has been presented elsewhere [42]. Instead, we limit ourselves to stating the final result

$$\dot{\rho} = \frac{-i}{\hbar}[H + H_{dd}, \rho] + \mathcal{L}_D\rho. \tag{2}$$

Here, ρ is the reduced density operator for the two atoms and H_{dd} is the dipole-dipole interaction Hamiltonian

$$H_{dd} = \frac{\hbar\gamma_0}{2}V_{dd}(qr)[\hat{\sigma}_1^+\hat{\sigma}_2^- + \hat{\sigma}_1^-\hat{\sigma}_2^+], \tag{3}$$

where γ_0 is the spontaneous decay rate of the transition and $\hat{\sigma}_i^+, \hat{\sigma}_i^-$ are usual raising and lower atomic operators for the ith atom. In view of the fact that the dipole-dipole interaction has the same physical origin as spontaneous emission, it is not surprising that it should scale as γ_0. The spatial part of the dipole-dipole interaction depends on the distance r between the two-level atoms, and is explicitly given by

$$V_{dd}(qr, \Theta) = -\frac{3}{2}\left[\frac{\cos qr}{qr}(1 - \cos^2\Theta) - \left(\frac{\sin qr}{(qr)^2} + \frac{\cos qr}{(qr)^3}\right)(1 - 3\cos^2\Theta)\right], \tag{4}$$

where Θ is the angle between the atomic dipoles and the relative position vector of the atoms $\mathbf{r}_2 - \mathbf{r}_1$. The divergence of $V_{dd}(qr, \Theta)$ as $r \to 0$ is an artifact of our oversimplified model and needs to be removed by an appropriate cutoff, as further discussed in Sec. III. The damping part of the master equation (2) is given by the Lindblad form

$$\mathcal{L}_D\rho = -\frac{3\gamma_0}{4}\int \frac{d\Omega}{4\pi}[\hat{\sigma}^+\hat{\sigma}^-\rho + \rho\hat{\sigma}^+\hat{\sigma}^- - 2\hat{\sigma}^-\rho\hat{\sigma}^+] , \quad (5)$$

where $d\Omega$ is a solid angle element, the surface integration is over a sphere of unit radius, and

$$\begin{aligned}\hat{\sigma}^-(\mathbf{k}) &= \left[\hat{\sigma}^+(\mathbf{k})\right]^\dagger \\ &= \sqrt{1-\cos^2\theta_k}[\hat{\sigma}_1^- e^{i\mathbf{k}\cdot\hat{\mathbf{r}}_1} + \hat{\sigma}_2^- e^{i\mathbf{k}\cdot\hat{\mathbf{r}}_2}]. \end{aligned} \quad (6)$$

The square root in this expression accounts for the dipole radiation pattern of a two-level system driven by a linearly polarized field, θ_k being the angle between the direction of the atomic dipole and the direction of emission of a spontaneous photon of wave vector $\mathbf{k}$.

Before turning to the Monte Carlo wave functions implementation of our model, we conclude this section by introducing a local basis that will prove useful to discuss our results. When analyzing the superradiant properties of two atoms at rest, Dicke [43] introduced the triplet and singlet states

$$\begin{aligned}|T_+\rangle &= |e\rangle_1 \otimes |e\rangle_2, \\ |T_-\rangle &= |g\rangle_1 \otimes |g\rangle_2, \\ |T_0\rangle &= (1/\sqrt{2})[|e\rangle_1 \otimes |g\rangle_2 + |g\rangle_1 \otimes |e\rangle_2], \\ |S_0\rangle &= (1/\sqrt{2})[|e\rangle_1 \otimes |g\rangle_2 - |g\rangle_1 \otimes |e\rangle_2], \end{aligned} \quad (7)$$

where the singlet state $|S_0\rangle$ is radiatively decoupled from the triplet family for atoms at rest at the same location. We generalize this basis set to account for the atomic center-of-mass motion by introducing the complete, symmetrized basis set

$$\begin{aligned}|U_1\rangle &= (1/\sqrt{2})[|x_1\rangle_1 \otimes |x_2\rangle_2 + |x_2\rangle_1 \otimes |x_1\rangle_2] \otimes |T_+\rangle , \\ |U_2\rangle &= (1/\sqrt{2})[|x_1\rangle_1 \otimes |x_2\rangle_2 + |x_2\rangle_1 \otimes |x_1\rangle_2] \otimes |T_-\rangle , \\ |U_3\rangle &= (1/\sqrt{2})[|x_1\rangle_1 \otimes |x_2\rangle_2 + |x_2\rangle_1 \otimes |x_1\rangle_2] \otimes |T_0\rangle , \\ |U_4\rangle &= (1/\sqrt{2})[|x_1\rangle_1 \otimes |x_2\rangle_2 - |x_2\rangle_1 \otimes |x_1\rangle_2] \otimes |S_0\rangle. \end{aligned} \quad (8)$$

Neglecting for now the kinetic energy contribution to the system's Hamiltonian, which leads to nonlocal dynamics, and introducing the vector $\mathbf{U} = (U_1, U_2, U_3, U_4)$, the local contribution to the Schrödinger evolution of $\mathbf{U}$ may be cast in the matrix form

$$i\hbar\dot{\mathbf{U}} = H_{loc}\mathbf{U} , \quad (9)$$

where

$$H_{loc} = \hbar\begin{pmatrix} -\delta & 0 & \mathcal{K}_+ & -\mathcal{K}_- \\ 0 & \delta & \mathcal{K}_+ & \mathcal{K}_- \\ \mathcal{K}_+ & \mathcal{K}_+ & \mathcal{D} & 0 \\ -\mathcal{K}_- & \mathcal{K}_- & 0 & -\mathcal{D} \end{pmatrix}, \quad (10)$$

$$\mathcal{K}_+ = \sqrt{2}\mathcal{R}\cos(qx_c)\cos(qx_r/2), \quad (11)$$

$$\mathcal{K}_- = \sqrt{2}\mathcal{R}\sin(qx_c)\sin(qx_r/2), \quad (12)$$

and

$$\mathcal{D} = (\gamma_0/2)V_{dd}(q|x_r|). \quad (13)$$

Here $x_r = x_1 - x_2$ is the projection along the axis of the standing wave of the relative position of the atoms, while $x_c = (x_1 + x_2)/2$ is the projection of their center-of-mass motion.

We see, then, that the interaction with the standing wave couples the electronic triplet state $|T_+\rangle$ to $|T_0\rangle$, and $|T_0\rangle$ to $|T_-\rangle$, with the effective Rabi frequency $\mathcal{K}_+$. In addition, it couples the singlet state $|S_0\rangle$ to the triplet states $|T_+\rangle$ and $|T_-\rangle$ with effective Rabi frequencies $\pm\mathcal{K}_-$. For atoms at the same location, $x_r = 0$, we have $\mathcal{K}_- = 0$ and hence recover Dicke's result that the singlet state decouples from the triplet manifold. In addition, the dipole-dipole interaction leads to a shift in energy of the electronic states $|S_0\rangle$ and $|T_0\rangle$. Since the strength of the dipole-dipole interaction scales with the spontaneous decay rate, this shift can be, and often is, considerably larger than the effective Rabi frequencies $\mathcal{K}_\pm$, a property that will prove useful in interpreting our numerical results.

III. MONTE CARLO WAVE FUNCTION SIMULATIONS

A direct numerical solution of the master equation (2) is beyond the capabilities of most present-day computers, due to prohibitive memory requirements. We chose instead to solve it using an equivalent Monte Carlo wave functions approach. This technique is now well documented [35,36], and we limit ourselves to a discussion of those aspects particular to the problem at hand. Since the dissipative part of the master equation is of the Lindblad form, it is possible to express Eq. (2) in the form

$$\dot{\rho} = \frac{-i}{\hbar}\left(H_{eff}\rho - \rho H_{eff}^\dagger\right) + \sum_m C_m\rho C_m^\dagger, \quad (14)$$

where

$$H_{eff} = H + H_{dd} - \frac{i\hbar}{2}\sum_m C_m^\dagger C_m \quad (15)$$

and the operators C_m are given by

$$C_m = \sqrt{\frac{3\gamma_0}{2}}\hat{\sigma}^-(\mathbf{k}). \quad (16)$$

This decomposition permits us to perform Monte Carlo wave function simulations as discussed, e.g., in Ref. [36]. The evolution of the wave function is governed by H_{eff} until a random quantum jump occurs; averaging over many runs then reproduces the results of the master equation.

Since from the definition (6), the operators C_m act on the two-particle space, some care is required in explicitly evaluating H_{eff}. We find that in addition to the usual spontaneous decay term, there is an additional contribu-

tion in the form of an imaginary potential, which results from the interference of spontaneous emission probability amplitudes due to the undistinguishability of the two particles. This prevents us knowing from which particle a detected photon was spontaneously emitted, and may be loosely interpreted as meaning that a particle decaying from its excited state at a given location can reappear in its ground state at the location of the other particle. Taking this term into account, we have

$$-\frac{i\hbar}{2}\sum_m C_m^\dagger C_m = -\frac{i\hbar\gamma_0}{2}[\hat{\sigma}_1^+\hat{\sigma}_1^- + \hat{\sigma}_2^+\hat{\sigma}_2^- + V_i(qr)(\hat{\sigma}_1^+\hat{\sigma}_2^- + \hat{\sigma}_1^-\hat{\sigma}_2^+)], \quad (17)$$

where

$$V_i(qr,\Theta) = j_0(qr) - \frac{1-3\cos^2\Theta}{2} j_2(qr), \quad (18)$$

the functions $j_i(x)$ being spherical Bessel functions of the first kind [44].

We noted earlier that $V_{dd}(qr,\Theta)$ diverges for $x_c \to 0$. To avoid this singularity in the numerical simulations, we resort to the fact that even for moderate atomic beam densities, the average interatomic separation $\langle r\rangle$ is quite large. For instance, for a density of 10^{12} cm^{-3}, we have $\langle r\rangle \simeq 10^{-4}$ cm, which is about two optical wavelengths, and interatomic separations smaller than, say, one tenth of a wavelength are extremely rare. We, therefore, introduce a cutoff by assuming a minimum interatomic distance r_0, and truncating the dipole-dipole interaction accordingly. Specifically, we fix the atomic separation in the direction of propagation of the atomic beam at this minimum distance r_0, but leave the motion in the quantized direction unconstrained. With this ansatz, the explicit forms of r and Θ in the potentials $V_{dd}(qr)$ and $V_i(qr)$ become

$$r = \sqrt{r_0^2 + x^2} \quad (19)$$

and

$$\cos^2\Theta = \frac{r_0^2}{r_0^2 + x^2}, \quad (20)$$

respectively, where we have assumed that the polarization vector of the standing wave is parallel to the z axis, the direction of the atomic beam.

The effective Hamiltonian (15) is used to evolve the wave function by means of a split-operator technique. At each time step, the evolution due to the Hamiltonian (1) is carried out using the band structure of the atoms interacting with the periodic standing-wave field; this is a straightforward generalization to two atoms of the band theory of Ref. [45]. The evolution due to the remaining part $H_{dd} - \frac{i\hbar}{2}\sum_m C_m^\dagger C_m$ of the effective Hamiltonian (15) is performed after transforming to the coordinate representation, where it is local. The time steps are limited on the one hand by the Monte Carlo technique, which requires that the exponential decay be well approximated by a first order expansion in Δt, and on the other hand by the split-operator technique, which requires that the two operations approximately commute. In practice the first of these constraints, $\gamma_0\Delta t \ll 1$, is the more restrictive one.

IV. RESULTS

To guide our thinking, we first examine the local Hamiltonian (10). Its diagonalization yields a set of four potentials $E_i(x_r,x_c)$, $i = 1,\ldots,4$, which are useful to gain an intuitive picture of the system dynamics, despite the fact that it neglects both the atomic motion and nonadiabatic transitions resulting from the kinetic energy. Figure 1(a) shows its local eigenvalues as a function of the relative position x_r of the atoms, for $x_c = 0$. In this example, $\mathcal{R} = 20\omega_{rec}$, $\delta = 0$, $\gamma_0 = 5000\omega_{rec}$, and the cutoff distance is $r_0 = \lambda$. (Because of the weak dependence of $E_i(x_r,x_c)$ on x_c, it is sufficient to consider the dependence of the local potentials on x_r in our qualitative discussion of the numerical results.) Note in particular the narrow avoided crossings between the eigenvalues E_1 and E_3 at $x_r \simeq 0.8\lambda$ and $x_r \simeq 1.4\lambda$. Figures 1(b)–1(d) are the projections $|\langle T_i|e_j\rangle|^2$ of the Dicke states $|T_+\rangle$, $|T_-\rangle$, $|T_0\rangle$, onto the eigenstates $|e_j(x_r,x_c)\rangle$, $j = 1,\ldots,4$, corresponding to $E_i(x_r,x_c)$, while Fig. 1(e) gives the probabilities $|\langle S_0|e_j\rangle|^2$. In these figures, the radius of the circles is proportional to the corresponding probabilities.

Consider for the sake of concreteness the relative distance $x_r = 0.65\lambda$. Here, the local potential E_1 is repulsive, and the corresponding eigenstate $|e_1\rangle$ is almost entirely composed of the Dicke state $|S_0\rangle$. In contrast, the local potential E_4 is binding, with $|e_4\rangle \simeq |T_0\rangle$. Hence, one might expect that an atomic system described by a wave packet initially confined near $x_r = 0.65\lambda$, and in the middle triplet state $|T_0\rangle$, would be bound by the dipole-dipole interaction. That this is indeed the case is illustrated in Fig. 2, which shows the evolution of an atomic system whose initial wave function is a symmetrized wave packet composed of two Gaussians peaked at 0.325λ and -0.325λ, and of equal widths $\sigma = 0.035\lambda$. The fact that the extent of the atomic wave function is small compared to an optical wavelength indicates that we are in the Stern-Gerlach regime of the near-resonant Kapitza-Dirac effect [46]. Plotted in the various curves is the marginal probability density

$$P(x_r) = \int dx_c |\psi(x_r,x_c)|^2 \quad (21)$$

of having the particles separated by the distance x_r, independently of the center-of-mass position of the system. Figure 2(a) shows the time evolution of the atomic system in the absence of any interaction, that is, neglecting both the standing-wave field and the dipole-dipole interaction. Spontaneous emission is also ignored in this example. As should be expected, the atomic evolution is fully determined by free space diffusion. In Fig. 2(b), the light field is turned on, but the dipole-dipole interaction and spontaneous emission are still neglected. This situation is essentially the same as that of Ref. [39], where the only many-body effect is in the symmetrization of the initial atomic wave function, except that we are now in

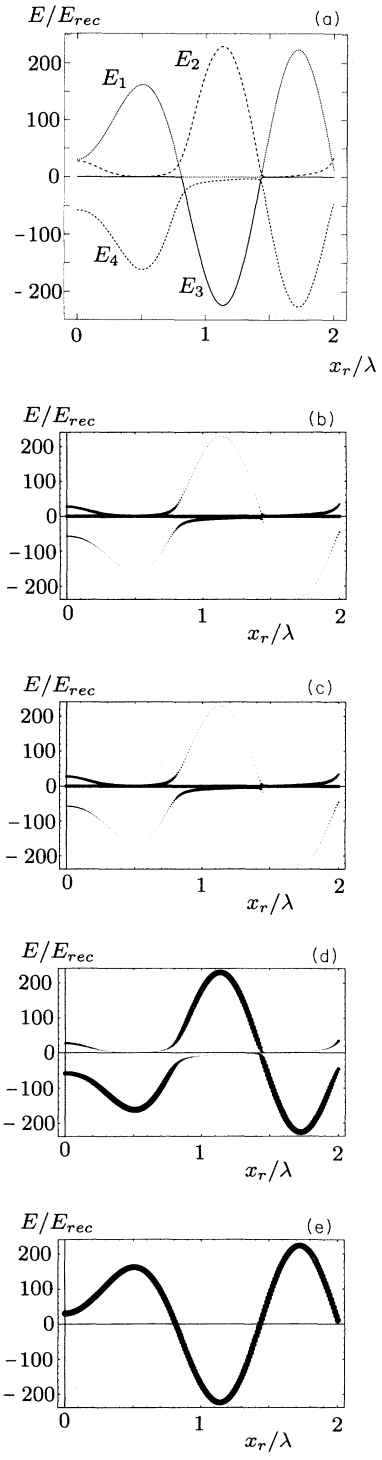

FIG. 1. (a) Eigenvalues $E_i(x_r, x_c), i = 1, \ldots, 4$ of the local Hamiltonian (10), versus the dimensionless relative atomic distance x_r/λ for $x_c = 0$. In this example, $\mathcal{R} = 20\omega_{rec}$, $\delta = 0$, $\gamma_0 = 5000\omega_{rec}$, and $r_0 = \lambda$; (b)–(d) Projections $|\langle T_i|e_j\rangle|^2$ of the Dicke states $|T_+\rangle$, $|T_0\rangle$, and $|T_-\rangle$, respectively, over the eigenstates $|e_j(x_r, x_c = 0)\rangle$ corresponding to the local potentials $E_j(x_r, x_c = 0)$; (e) Projections $|\langle S_0|e_j\rangle|^2$ of the Dicke state $|S_0\rangle$ over the local eigenstates $|e_j(x_r, x_c = 0)\rangle$. In these figures, the radii of the circles is proportional to the corresponding probabilities.

the Stern-Gerlach rather than the Raman-Nath regime of diffraction, and observe, therefore, the oscillations characteristic of this regime. The effects of the dipole-dipole potential are clearly evident in Figs. 2(c)–2(e). In the case where the initial electronic state is the middle triplet $|T_0\rangle$, we observe a strong binding of the atoms in the potential $E_4(x_r, x_c)$. The atomic system always remains in the vicinity of the minimum of that potential, never approaching any other potential surface. This is further confirmed by Fig. 2(d), which shows the populations of the various Dicke states as a function of time. As expected, they remain roughly constant in that case.

In contrast, Fig. 2(e) shows what happens if the atoms are initially in the electronic singlet state $|S_0\rangle$. In this case, the atoms experience the repulsive potential $E_1(x_r, x_c)$, the atomic wave function starts "rolling down the hill" and rapidly approaches the narrow avoided crossings at $x_r \simeq 0.8\lambda$ and $x_r \simeq 1.4\lambda$. The branching of the atomic wave function into these potential surfaces is clearly evident in Fig. 3(a), which shows a short-time close-up of Fig. 2(e). These nonadiabatic transitions are further illustrated in Fig. 3(b), which shows how the atomic population leaves the initial local eigenstate.

While the results of Figs. 2 and 3 are easily understood in terms of local potentials and are quite useful from a pedagogical point of view, one should keep in mind that they were obtained at resonance $\delta = 0$, and hence are expected to be strongly influenced by spontaneous emission. Rather than pursuing this example further, we now turn to another situation, where the field is detuned from the atomic transition frequency. As we shall see, this presents the double advantage of reducing somewhat the effects of spontaneous emission, and of leading to the existence of minima of the local potential near $x_r = 0$. Figure 4 shows the local eigenstates of the Hamiltonian (10) for $\mathcal{R} = 500\omega_{rec}$ and $\delta = -1000\omega_{rec}$. (In the absence of dipole-dipole interaction, the four local eigenvalues of the dressed atoms consist of two periodic potentials and two degenerate constant potentials, the periodic potentials corresponding to the approximate eigenstates $|T_-\rangle$ and $|T_+\rangle$ for large detunings.) Figures 4(a) and 4(b) show the projections $|\langle T_-|e_j\rangle|^2$ and $|\langle T_0|e_j\rangle|^2$ of the Dicke states $|T_-\rangle$ and $|T_0\rangle$, respectively, onto the eigenstates $|e_j(x_r, x_c = 0)\rangle$, $j = 1, \ldots, 4$. The other two projections are not shown, as they are only weakly populated and play no major role in the subsequent discussion.

Consider for concreteness a situation where the atoms are initially in the $|T_-\rangle$ state, with symmetrized Gaussian coordinate representation wave functions peaked at $\pm\lambda/8$ and of equal widths $\sigma = 0.025\lambda$. Figure 5(a) shows the resulting time evolution of the marginal probability density

$$P(x_1) = \int dx_2 |\psi(x_1, x_2)|^2 \tag{22}$$

for one of the atoms to be at position x_1 as a function of time, under the influence of the light field alone. This is once more the usual optical Stern-Gerlach effect [46]. The modifications to the dynamics brought about by

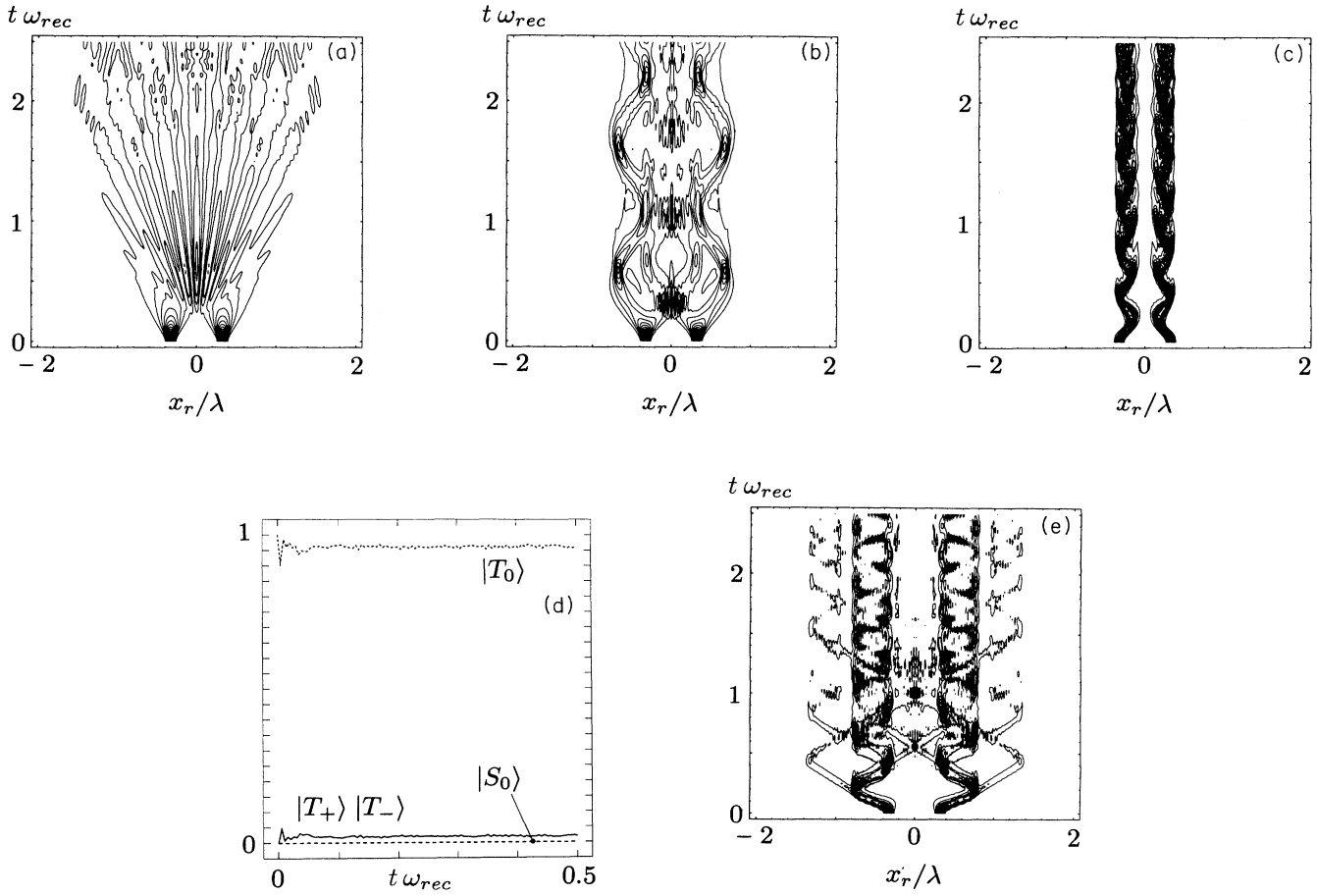

FIG. 2. Marginal probability density $P(x_r,t) = \int dx_c |\psi(x_r,x_c,t)|^2$ for a two-atom system initially in the $|T_0\rangle$ Dicke state (a)–(d) and in the $|S_0\rangle$ state (e). 2(d) shows the corresponding evolution of the Dicke states. In all cases, the system is on resonance, $\delta = 0$, spontaneous emission is ignored, and the time is in units of ω_{rec}^{-1}; (a) both the standing-wave field and the dipole-dipole interaction are neglected; (b) A standing wave with $\mathcal{R} = 20\omega_{rec}$ is included, but the dipole-dipole interaction is neglected; (c)–(d) The dipole-dipole interaction is also included, with $\gamma_0 = 5000\omega_{rec}$ and $r_0 = 1.0\lambda$.

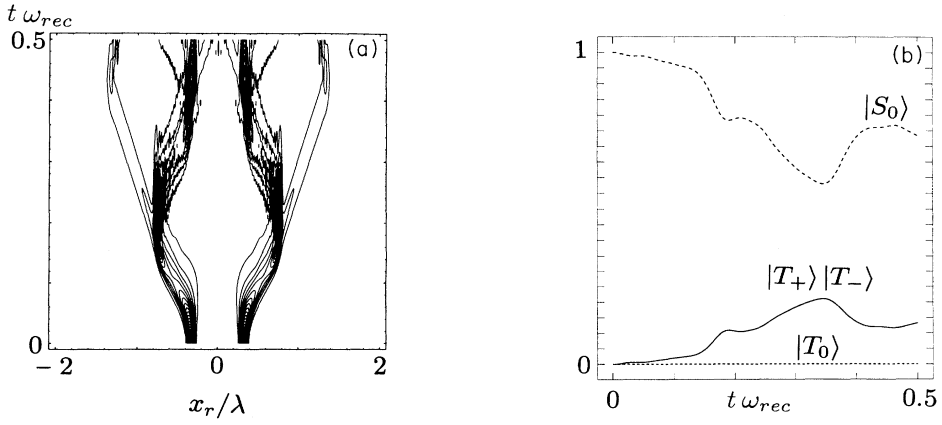

FIG. 3. (a) Expanded view of the early evolution of Fig. 2(e); (b) Evolution of the various Dicke state populations for the case of Fig. 2(e). Time in units of ω_{rec}^{-1}.

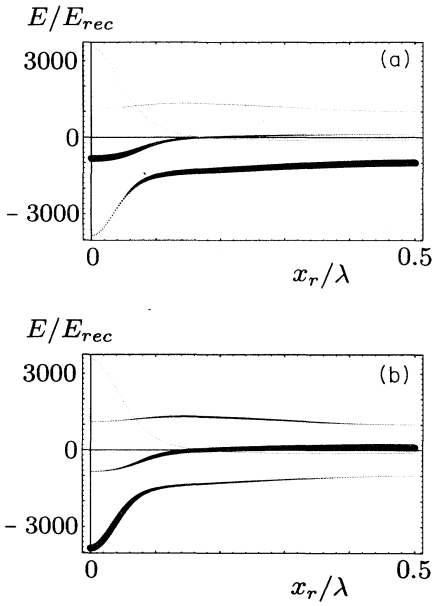

FIG. 4. Projections (a) $|\langle T_-|e_j\rangle|^2$ and (b) $|\langle T_0|e_j\rangle|^2$ of Dicke states $|T_-\rangle$ and $|T_0\rangle$ over the eigenstates $|e_j(x_r, x_c = 0)\rangle$ corresponding to the local potentials $E_j(x_r, x_c = 0)$ for $\mathcal{R} = 500\omega_{rec}$, $\delta = -1000\omega_{rec}$, $\gamma_0 = 500\omega_{rec}$, and $r_0 = 0.1\lambda$.

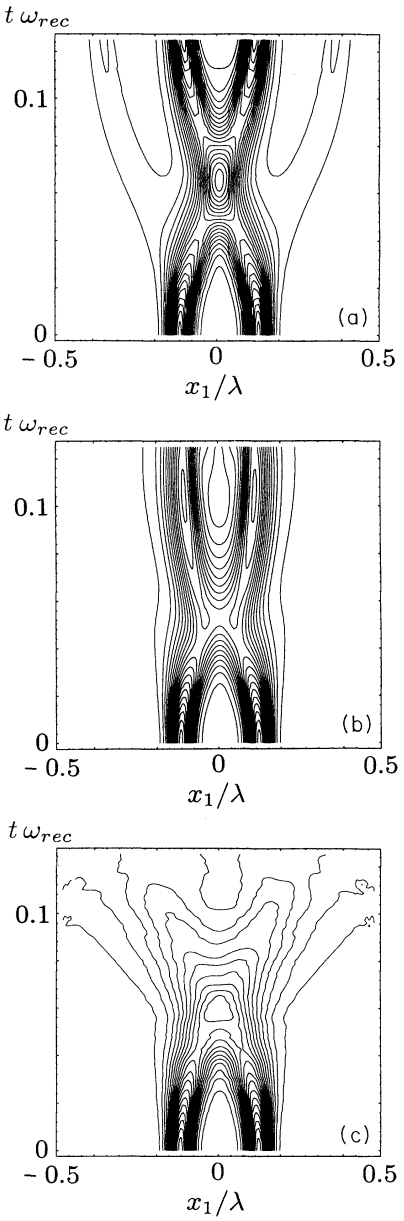

FIG. 5. Time evolution of the marginal probability density $P(x_1, t) = \int dx_2 |\psi(x_1, x_2, t)|^2$ for the parameters of Fig. 4 as a function of the dimensionless time $\omega_{rec}t$; (a) dipole-dipole interaction and spontaneous ignored; (b) spontaneous emission ignored; (c) spontaneous emission also included.

the dipole-dipole interaction are illustrated in Fig. 5(b), where spontaneous emission has, however, been ignored. This result can be physically understood in conjunction with Fig. 6, which shows the populations of the various Dicke levels as a function of time. For short enough times, the atomic population oscillates primarily between the Dicke states $|T_-\rangle$ and $|T_0\rangle$ at the difference frequency between the potentials E_{-1} and E_0, see Fig. 4(b). These Rabi-like oscillations are merely due to the fact that the initial state $|T_-\rangle$ is not an eigenstate of the system.

In addition to these oscillations, there is also a change in Dicke state populations due to the fact that their projection onto the various eigenstates is a function of the relative coordinate x_r. For instance, the local eigenstates corresponding to the local potential $E_4(x_r, x_c)$ is primarily composed of the Dicke state $|T_-\rangle$ at large x_r, and of the Dicke state $|T_0\rangle$ at short distances. This leads to an adiabatic evolution whose signature is still apparent near the time $t = 5 \times 10^{-2}\omega_{rec}^{-1}$. In addition, nonadiabatic transitions due to the kinetic energy of the atoms are also taking place, but it is difficult to identify their effects separately in the present example.

Figure 5(b) clearly shows that as a result of this rather complicated dynamics ("Rabi-type" oscillations, adiabatic transitions, and nonadiabatic transitions), the atomic system appears to remain bound by the combined effects of the electric dipole and dipole-dipole interaction for reasonably long times, the relative distance between the atoms in this "dipole-dipole molecule," or "diatom," being of the order of half an optical wavelength. In some sense, this may be understood as the two-atom bound state corresponding to the many-body soliton solutions predicted in nonlinear atom optics [31,33]. This correspondance is however somewhat tenuous, since nonlinear atom optics deals with the effective dynamics of a single atom in the mean field provided by the others, and hence the concept of relative coordinate loses its meaning there, a well-known symmetry-breaking feature of the Hartree-Fock approximation [47].

Atomic solitons have recently been found not to survive the effects of spontaneous emission [48], and it is interesting to determine whether the situation is similar

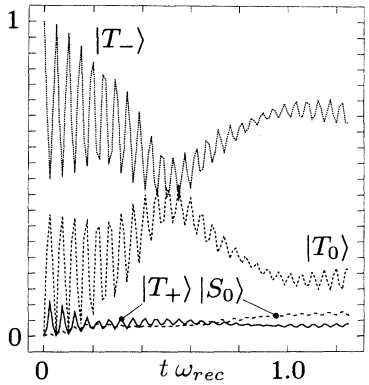

FIG. 6. Populations of the various Dicke levels as a function of the dimensionless time $\omega_{rec}t$ for the situation of Fig. 5(b).

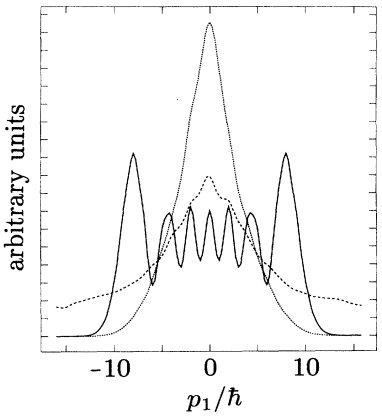

FIG. 7. Marginal momentum probability distribution $P(p_1) = \int dp_2 |\psi(p_1, p_2)|^2$ in the Raman-Nath regime, after an interaction time $t = 0.1\omega_{rec}^{-1}$. The relevant parameters are $\mathcal{R} = 100\omega_{rec}$, $\delta = 0$, $\gamma_0 = 100\omega_{rec}$, and $r_0 = 0.1\lambda$. Solid line: spontaneous emission and dipole-dipole force neglected; dotted line: spontaneous emission included, but dipole-dipole interaction neglected; dashed line: dipole-dipole interaction included.

here. Figure 5(c) shows the same example as in Fig. 5(b), but with spontaneous emission included. We see that indeed, this incoherent process rapidly destroys the bound state. This can be qualitatively understood in terms of the local potentials of Fig. 4. As the atoms undergo their collision, they reach a relative distance where the lowest local potential is quite steep, and the corresponding eigenstate is mostly composed of the $|T_0\rangle$ Dicke state, see Fig. 4(b). When in this state, the atoms are strongly susceptible to spontaneous emission, thereby winding up in the local potential E_3, whose corresponding eigenstate $|e_3\rangle \simeq |T_-\rangle$. However, while falling down the potential well $E_4(x_r)$, the atoms can gain a substantial amount of kinetic energy, which can in turn be used to expel the atoms from the shallower well $E_3(x_r)$. This heating mechanism is somewhat reminiscent of laser heating in a strong standing wave with red detuning [49]. An important difference between the two situations is that in strong-field Sysiphus cooling or heating, the two potentials between which the atom jumps have identical curvatures, but are shifted by a half wavelength. In contrast, the present heating utilizes the difference in curvature between the two potentials involved. The possibility of using similar techniques to achieve cooling are presently under study.

As a final example, we look at the effect of the dipole-dipole force on atomic diffraction in the Raman-Nath regime, which has previously been extensively studied both experimentally and theoretically [1,2] in the single-atom case. In contrast to the Stern-Gerlach regime, we now consider initial wave functions with spatial extensions on the order of or larger than an optical wavelength λ. We proceed numerically by incoherently averaging results obtained over many initial positions, thereby simulating the experimental situation of an atomic beam with well defined momentum. We specifically concentrate on the evolution of the marginal momentum distribution of one of the atoms,

$$P(p_1) = \int dp_2 |\psi(p_1, p_2)|^2, \tag{23}$$

which, on leaving the interaction region and propagating to the far field, becomes the experimentally detected position distribution. In the absence of spontaneous emission, the standing-wave field scatters the momentum wave function in units of $\hbar q$, leading to well separated diffraction orders whose amplitude is given by a well-known Bessel function distribution [50]. Spontaneous emission can be minimized by ensuring that the excited state population remains negligible, for example by working far off resonance. When there is substantial spontaneous emission, the diffraction orders are washed out, since the atomic recoil from the emitted photon is randomly distributed [1,3,4]. Since the near-resonant dipole-dipole interaction and spontaneous emission have the same physical origin, the study of its effect on Raman-Nath diffraction requires one to work in this diffusion-dominated regime. Figure 7 shows $P(p)$ for a choice of parameters corresponding to the experimental situation of Ref. [1]. The solid line shows for reference the result of Raman-Nath diffraction in the absence of spontaneous emission, the width of the various diffraction orders being due to the width of the incident atomic beam. The dotted line shows the effects of spontaneous emission on this pattern, with the well-known transition from a diffractive to a diffusive regime [1,3,4]. The effects of the dipole-dipole interaction are insignificant if the cutoff distance $r_0 \geq \lambda$, and lead to a result practically identical to the dotted line. Indeed, large densities are required to observe significant effects, as illustrated by the dashed line, which corresponds to a cutoff distance $r_0 = 0.1\lambda$. Such a short cutoff distance implies an unrealistic density of about 10^{15} cm^{-3}. As a final remark, we note that the Raman-Nath results can clearly not be simply interpreted in terms of the local potentials $E_i(x_r, x_c)$, due to the strongly delocalized nature of the atomic wave functions.

V. CONCLUSION

In this paper, we have applied an effective one-dimensional model to the study of the near-resonant Kapitza-Dirac diffraction of two atoms interacting via the dipole-dipole interaction. We have concentrated mostly on the Stern-Gerlach regime of diffraction, where the atomic wave functions are sufficiently well localized that a good physical understanding of the atomic dynamics in terms of local potentials can be achieved. In general, the dipole-dipole interaction is found to lead to substantial modifications of the Stern-Gerlach diffraction patterns even for large cutoff distances $r_0 \simeq \lambda$, which correspond to atomic densities of the order of 10^{10} cm^{-3}. We found that under appropriate conditions, bound states of the atomic system can be achieved, with the two atoms separated by a distance of the order of hundreds of nanometers. However, spontaneous emission eventually destroys the binding between these states via a heating mechanism somewhat similar to strong-field Sysiphus heating. In this respect, the behavior of the diatom bound state under the influence of spontaneous emission is similar to that of the atomic solitons predicted to occur in near-resonant Kapitza-Dirac diffraction in the framework of nonlinear atom optics.

Our present model suffers from a number of weaknesses, that we are presently proceeding to remove: most important amongst them are the effective one-dimensional model and the use of two-level atoms. In addition, we are investigating whether the heating resulting from the dipole-dipole interaction can be turned around and changed into a cooling and/or confining mechanism.

ACKNOWLEDGMENTS

This work is funded by the U.S. Office of Naval Research Contract No. N00014-91-J1205, by the National Sciences Foundation Grant No. PHY92-13762, and by the Joint Services Optics Program.

[1] P. L. Gould, P. J. Martin, G. R. Ruff, R. E. Stoner, J.-L. Picqué, and D. E. Pritchard, Phys. Rev. A **43**, 585 (1991).
[2] For a detailed theoretical discussion of the near resonant Kapitza-Dirac effect, see e.g., E. Schumacher, M.Wilkens, P. Meystre, and S. Glasgow, Appl. Phys. B **54**, 451 (1992).
[3] S. M. Tan and D. F. Walls, Phys. Rev. A **44**, 2779 (1991).
[4] M. Wilkens, E. Schumacher, and P. Meystre, Opt. Commun. **86**, 34 (1991).
[5] P. Meystre, E. Schumacher, and S. Stenholm, Opt. Commun. **73**, 443 (1989).
[6] P. Storey, M. Collett, and D. F. Walls, Phys. Rev. Lett. **68**, 472 (1992).
[7] M. Marte and P. Zoller, Appl. Phys. B **54**, 477 (1992).
[8] A. M. Herkommer, V. M. Akulin, and W. P. Schleich, Phys. Rev. Lett. **69**, 3298 (1992).
[9] I. Sh. Averbukh, V. M. Akulin, and W. P. Schleich, Phys. Rev. Lett. **72**, 437 (1994).
[10] A. Aspect, E. Arimondo, R. Kaiser, N. Vansteenkiste, and C. Cohen-Tannoudji, Phys. Rev. Lett. **61**, 826 (1988).
[11] M. Kasevich and S. Chu, Phys. Rev. Lett. **69**, 1741 (1992).
[12] See e.g., T. J. Greytak and D. Kleppner, in *New Trends in Atomic Physics*, edited by G. Grynberg and R. Stora (North-Holland, Amsterdam, 1984).
[13] R. R. McLone and E. A. Power, Mathematika **11**, 91 (1964).
[14] R. R. McLone and E. A. Power, Proc. R. Soc. London, Ser. A **286**, 573 (1965).
[15] A. Gallagher and D. E. Pritchard, Phys. Rev. Lett. **63**, 957 (1989).
[16] P. S. Julienne and J. Vigué, Phys. Rev. A **44**, 4464 (1991).
[17] A. M. Smith and K. Burnett, J. Opt. Soc. Am. B **8**, 1592 (1991).
[18] Y. B. Band and P. S. Julienne, Phys. Rev. A **46**, 330 (1992).
[19] C. D. Wallace, T. P. Dinnen K.-Y. N. Tan, T. T. Grove, and P. L. Gould, Phys. Rev. Lett. **69**, 897 (1992).
[20] C. R. Monroe, E. A. Cornell, C. A. Sackett, C. J. Myatt, and C. E. Wieman, Phys. Rev. Lett. **70**, 414 (1993).
[21] L. Marcassa, V. Bagnato, Y. Wang, C. Tsao, J. Weiner, O. Dulieu, Y. B. Band, and P. S. Julienne, Phys. Rev. A **47**, R4563 (1993).
[22] K. Ellinger, J. Cooper, and P. Zoller, Phys. Rev. A **49**, 3909 (1994).
[23] K.-A. Suominen, M. J. Holland, K. Burnett, and P. S. Julienne, Phys. Rev. A **49**, 3897 (1994).
[24] M. J. Holland, K.-A. Suominen, and K. Burnett, Phys. Rev. Lett. **72**, 2367 (1994).
[25] B. Svistunov and G. Shlyapnikov, Zh. Eksp. Teor. Fiz. **97**, 821 (1990) [Sov. Phys. JETP **97**, 460 (1990)].
[26] B. Svistunov and G. Shlyapnikov, Zh. Eksp. Teor. Fiz. **98**, 129 (1990) [Sov. Phys. JETP **98**, 129 (1990)].
[27] H. D. Politzer, Phys. Rev. A **43**, 6444 (1991).
[28] J. Javanainen, Phys. Rev. Lett. **72**, 2375 (1994).
[29] M. Lewenstein and L. You, Phys. Rev. Lett. **71**, 1339 (1993).
[30] W. Zhang and D. F. Walls, Quantum Opt. **5**, 9 (1993).
[31] G. Lenz, P. Meystre, and E. W. Wright, Phys. Rev. Lett. **71**, 3271 (1993).
[32] W. Zhang, D. F. Walls, and B. C. Sanders, Phys. Rev. Lett. **72**, 60 (1994).
[33] G. Lenz, P. Meystre, and E. M. Wright, Phys. Rev. A **50**, 1681 (1994).
[34] M. Lewenstein, L. You, J. Cooper, and K. Burnett, Phys. Rev. A **50**, 2207 (1994).
[35] H. J. Carmichael, in *An Open Systems Approach to Quantum Optics*, Lecture Notes in Physics New Series Vol. m18 (Springer-Verlag, Berlin, 1993).
[36] K. Mølmer, Y. Castin, and J. Dalibard, J. Opt. Soc. Am. B **10**, 524 (1993).

[37] E. Goldstein, P. Pax, K. Schernthanner, B. Taylor, and P. Meystre, Appl. Phys. B **60**, 161 (1995).
[38] J. Guo, Phys. Rev. A **50**, R2830 (1994).
[39] G. Lenz, P. Pax, and P. Meystre, Phys. Rev. A **48**, 1707 (1993).
[40] See e.g., C. Cohen-Tannoudji, J. Dupont-Roc, and G. Grynberg, *Photons and Atoms, Introduction to Quantum Electrodynamics* (Wiley, New York, 1989).
[41] See e.g., R. Graham and F. Haake, *Quantum Statistics in Optics and Solid-State Physics*, Springer Tracts in Modern Physics Vol. 66 (Springer, Berlin, 1973).
[42] G. Lenz and P. Meystre, Phys. Rev. A **48**, 3365 (1993).
[43] R. H. Dicke, Phys. Rev. **93**, 99 (1954).
[44] M. Abramowitz and I. A. Stegun, *Handbook of Mathematical Functions* (Dover, New York, 1972).
[45] M. Wilkens, E. Schumacher, and P. Meystre, Phys. Rev. A **44**, 3130 (1991).
[46] T. Sleator, T. Pfau, V. Balykin, O. Carnal, and J. Mlynek, Phys. Rev. Lett. **68**, 1996 (1992).
[47] A very clear discussion of this point can be found in R. Peierls, J. Phys. A **24**, 5273 (1991).
[48] G. Lenz, K. Schernthanner, and P. Meystre, Phys. Rev. A **50**, 4170 (1994).
[49] C. Cohen-Tannoudji, in *Fundametal Systems in Quantum Optics*, edited by J. Dalibard, J. M. Raimond, and J. Zinn-Justin (North-Holland, Amsterdam, 1992), p. 153.
[50] E. Arimondo, A. Bambini, and S. Stenholm, Phys. Rev. A **24**, 898 (1981).